

Paper I

C. Sætre, J. Stadsnes, H. Nesse, A. Aksnes, S. M. Petrinec, C. A. Barth, D. N. Baker, R. R. Vondrak, and N. Østgaard (2004)

Energetic electron precipitation and the NO abundance in the upper atmosphere: A direct comparison during a geomagnetic storm

J. Geophys. Res., 109, A09302, doi:10.1029/2004JA010485.

Energetic electron precipitation and the NO abundance in the upper atmosphere: A direct comparison during a geomagnetic storm

C. Sætre,¹ J. Stadsnes,¹ H. Nesse,¹ A. Aksnes,¹ S. M. Petrinec,² C. A. Barth,³ D. N. Baker,³ R. R. Vondrak,⁴ and N. Østgaard⁵

Received 19 March 2004; revised 13 May 2004; accepted 23 June 2004; published 8 September 2004.

[1] Nitric oxide (NO) densities at heights between 96 and 150 km in the Earth's upper atmosphere are directly compared with the energy deposition from precipitating energetic electrons. The comparisons are done for the beginning of a geomagnetic storm event on 2 May 1998. The electron energy is derived from X-ray bremsstrahlung observations from the Polar Ionospheric X-ray Imaging Experiment (PIXIE) on board the Polar spacecraft. Measurements of the NO density are performed by the Student Nitric Oxide Explorer (SNOE) on the dayside by measuring airglow spectral features of the NO γ -band. Since a significant part of the electron precipitation takes place during the night, and considering the long lifetime of NO, we have accumulated the X-ray data in geographical boxes. This enables us to follow the development of the total energy deposition over a specific area during the night and morning hours. In agreement with theoretical predictions we find an increase in NO at higher latitudes due to electron precipitation. At 106 km altitude, which is found to be the average altitude of the peak values of both NO intensity and precipitating electron energy, $\sim 83\%$ of the NO density is produced by electron precipitation. At this altitude we find that the electron precipitation results in the production of ~ 8 NO molecules per keV deposited energy. The comparison of the data also shows effects of a horizontal neutral wind. Above 100 km the peak in NO density is displaced equatorward of the peak in electron energy deposition.

INDEX TERMS: 2716 Magnetospheric Physics: Energetic particles, precipitating; 2736 Magnetospheric Physics: Magnetosphere/ionosphere interactions; 2437 Ionosphere: Ionospheric dynamics; 2407 Ionosphere: Auroral ionosphere (2704); 2455 Ionosphere: Particle precipitation; *KEYWORDS:* PIXIE, SNOE, nitric oxide, electron precipitation

Citation: Sætre, C., J. Stadsnes, H. Nesse, A. Aksnes, S. M. Petrinec, C. A. Barth, D. N. Baker, R. R. Vondrak, and N. Østgaard (2004), Energetic electron precipitation and the NO abundance in the upper atmosphere: A direct comparison during a geomagnetic storm, *J. Geophys. Res.*, 109, A09302, doi:10.1029/2004JA010485.

1. Introduction

[2] The effects in the upper atmosphere of solar and magnetospheric energetic particle precipitation have been studied for several decades. Among the chemical effects, the variations in ozone density are of particular interest. The connection between energetic particle precipitation and ozone is mainly through the production of HO_x and NO_x which destroy ozone in catalytic reactions. Nitric oxide (NO) is easily produced by energy input into the atmosphere. The NO density is highly variable, with maximum

density in the higher latitude regions at heights typically around 106 km altitude. The higher latitude portion of the NO abundance has been shown to vary with the intensity of the auroral precipitation [e.g., Barth, 1992]. Precipitating electrons with energy of ~ 10 keV deposit most of their energy at altitudes between ~ 100 and ~ 115 km [Rees, 1963], that is, the altitude region of maximum NO density.

[3] The main production mechanism of nitric oxide in the upper atmosphere is the reaction of excited nitrogen atoms with molecular oxygen. Energetic electrons, both photoelectrons produced by solar soft X rays and auroral precipitating electrons, produce excited atomic nitrogen atoms from the dissociative excitation of molecular nitrogen. The additional ionization also leads to the production of excited nitrogen atoms through the dissociative recombination of NO⁺ or N₂⁺. The main loss process of nitric oxide is photodissociation by solar ultraviolet radiation.

[4] The ozone layer in the stratosphere can be affected by the NO abundance in the lower thermosphere. The lifetime of NO is sufficiently long particularly during the winter, so that NO can be transported by vertical winds from the lower

¹Department of Physics and Technology, University of Bergen, Norway.

²Lockheed Martin Advanced Technology Center, Palo Alto, California, USA.

³Laboratory for Atmospheric and Space Physics, University of Colorado, Boulder, Colorado, USA.

⁴NASA/Goddard Space Flight Center, Greenbelt, Maryland, USA.

⁵Space Sciences Laboratory, U. C., Berkeley, California, USA.

thermosphere to the stratosphere [Solomon *et al.*, 1982]. This would work especially during winter when there is a substantial downward transport of air through the middle atmosphere at higher latitudes [Randall *et al.*, 2001; Callis and Lambeth, 1998; Callis *et al.*, 1996].

[5] Nitric oxide is also important for the heat balance in the upper atmosphere, as it radiates effectively in the infrared part of the spectrum. Owing to the low ionization threshold of NO the NO density controls the ion composition in the *E* region of the ionosphere. Ionization of NO by Lyman- α radiation causes NO⁺ to be one of the most dominant ions in the *D* region of the ionosphere.

[6] Production of nitric oxide due to solar soft X rays and electron precipitation has been studied [e.g., Baker *et al.*, 2001; Barth *et al.*, 1999, 2001, 2002, 2003; Callis *et al.*, 1998; Crowley *et al.*, 1998, 1999; Petrinec *et al.*, 2003; Ridley *et al.*, 1999; Roble, 1992; Solomon *et al.*, 1999] and modeled [e.g., Codrescu *et al.*, 1997; Bailey *et al.*, 2002; Barth, 1992; Siskind *et al.*, 1989]. Barth *et al.* [1999] compared simultaneous measurements of solar soft X rays and thermospheric nitric oxide. They found a 0.88 correlation in the tropics during low geomagnetic activity ($A_p < 10$). They concluded that the primary cause of the NO variability in the lower thermosphere in the tropics is the variability in the flux of the solar soft X rays. The NO density in the tropics has maximum value of $\sim 5 \times 10^7$ molecules/cm³.

[7] A statistical study of Petrinec *et al.* [2003] compared auroral bremsstrahlung X rays, as observed by the Polar Ionospheric X-ray Imaging Experiment (PIXIE), and nitric oxide density, as measured by the Student Nitric Oxide Explorer (SNOE). The study spanned over 3 years of data and the two data sets consisted of daily averages. Petrinec *et al.* [2003] found a rather modest correlation between the measurements, indicating that 20–40% of the variation in the high-latitude thermospheric nitric oxide was caused by the electron precipitation. The correlation was 0.57 when the NO observations were delayed one day with respect to the X-ray measurements. When also considering the seasonal effects on the NO density, the correlation coefficient increased from 0.57 to 0.63. However, Petrinec *et al.* [2003] stressed the difficulties of doing a statistical comparison, when the timescales change significantly with observational circumstances and with altitude.

[8] Baker *et al.* [2001] did a 2 year statistical study where the NO volume density, as measured by SNOE, was compared with energetic electron fluxes ($E > 25$ keV) from measurements by the Low-Energy Ion Composition Analyzer (LICA) instrument on board the Solar Anomalous Magnetospheric Particle Explorer (SAMPEX) satellite. In addition, the NO volume density was compared with the “hemispherical power index” (HPI) obtained by the National Oceanic and Atmospheric Administration (NOAA) TIROS satellites. When the seasonal variations in the NO density also were considered, the correlation coefficient was found to be between ~ 0.6 and ~ 0.7 for both comparisons. Baker *et al.* [2001] also compared NO measurements from SNOE and SAMPEX data for three geomagnetic storm events. They found a large latitudinal asymmetry between the winter and summer hemispheres in the NO production and that the NO profile was spread equatorward in latitude during major storms. The comparisons were made with daily averaged data.

[9] The present study compares directly the energy deposition from precipitating energetic electrons, and the increase in NO density at higher latitudes, during the beginning of a geomagnetic storm event on 2 May 1998. On the two days before this date the geomagnetic activity was low. The lifetime of NO is approximately 1 day [Barth *et al.*, 2003]. With quiet conditions prior to the storm, we can expect the abundance of NO at higher latitudes to be directly related to the electron precipitation during the storm.

[10] The UV spectrometer onboard SNOE measured the NO density in day light only, and the SNOE orbit crossed the equator at approximately 1030 local time (LT). Nitric oxide produced by electron precipitation during the night will have sufficiently long lifetime to rotate with the Earth over to the dayside. Here the NO density can be measured by SNOE. This means that we must take into account all the electron precipitation that takes place over a given area during the night and morning. Therefore the X-ray bremsstrahlung intensities are accumulated in geographical boxes. The measurements start some hours before the major storm activity 2 May 1998. We integrate the X-ray intensity over consecutive longer intervals of time and investigate the increase of NO during these hours.

2. Instrumentation

2.1. PIXIE (Polar Ionospheric X-Ray Imaging Experiment)

[11] PIXIE is an X-ray camera on board the Polar spacecraft [Imhof *et al.*, 1995]. The instrument is a pinhole camera with two separate gas proportional counters recording time, position, and energy for each incident X-ray photon in the energy range from ~ 2.5 to 22 keV. Owing to a high-voltage problem, the front chamber (2.5–9 keV) has to be duty-cycled. On 2 May 1998 it was switched on for ~ 4.5 min and off for ~ 5.5 min. However, the rear chamber (9–22 keV) provided continuous measurements. In order to obtain sufficient count rates to derive electron spectra from the X-ray measurements, we have integrated the X-rays from the front (rear) chamber for 4.5 (10) min with the same center time.

[12] The Polar spacecraft has a polar orbit with apogee at $\sim 9 R_E$. In May 1998 the apogee was above the northern polar regions, giving PIXIE a nearly global view of the auroral regions. The extensive coverage by PIXIE is highly valuable when comparing energetic electron precipitation and chemical changes, where the chemical component has a long lifetime.

2.2. SNOE (The Student Nitric Oxide Explorer)

[13] SNOE was a research satellite built and operated at the University of Colorado. SNOE measured the NO density in the lower thermosphere and analyzed the solar and magnetospheric effects on the NO abundance [Solomon *et al.*, 1996]. The satellite had a circular orbit at 550 km altitude, with 97.5° inclination. It was sun synchronous and crossed the equator at ~ 1030 LT on the dayside.

[14] An ultraviolet spectrometer (UVS) measured the NO density by observing the NO gamma band features (215 nm and 237 nm) in the dayglow. The intensity of the (0,1) gamma band at 237 nm was used to determine the density of NO [Barth *et al.*, 2003].

[15] Since the UVS observed the dayglow emissions, it measured the NO density on the dayside of the orbit, that is, at ~ 1030 LT. Areas that experienced electron precipitation during the night and early morning hours had to rotate with the Earth over to the dayside before the enhancements in NO could be observed by SNOE. It could take more than 10 hours before the chemical effect of a geomagnetic storm was observed by SNOE. With the time-integrated X-ray intensity in a geographical grid in latitude and longitude, we should have a good basis for comparing the data.

3. Observations

[16] In this study we investigate the connection between energetic electron precipitation and the abundance of NO in the upper atmosphere, during a magnetic storm on 2 May 1998. NO has a lifetime of approximately 1 day. The best conditions for comparison is a geomagnetic storm, where the geomagnetic conditions have been rather quiet during the preceding days. Then we can assume that an increase in the NO concentration in the auroral areas is connected to the measurements of the particle precipitation over the same geographical areas.

[17] As seen in Figure 1, the Dst index dropped from fairly quiet levels to ~ -80 nT on 2 May 1998. The AE index increased from quiet conditions to almost 2400 nT around noon that day, and we see a corresponding decrease in the AL index. This indicates a severe injection of electrons on the nightside from the plasma sheet. Since both the Dst and the AE index indicate quiet geomagnetic conditions on the days before 2 May 1998, this date is well suited for this comparison study.

[18] On 2 May 1998, we have PIXIE X-ray measurements between 0220 and 1245 UT. At 1245 UT the Polar spacecraft entered the radiation belts, wherein the PIXIE high-voltage is routinely switched off to protect the instrument against saturation due to in situ energetic particles. The observations from PIXIE start at 0220 UT 2 May 1998, several hours before the first onset at 0530 UT. Figure 2 shows the time-integrated X-ray intensity for X rays with energies between 2.47 and 9.06 keV. Integrating X rays from the front chamber we have assumed that the X-ray fluxes stayed constant during the 5.5 min it was turned off due to the duty cycling. The intensities are integrated over consecutive longer intervals of time. We compare with the NO measurements from nine SNOE passes, where the three last passes occurred after the PIXIE camera was turned off.

[19] The areas of largest X-ray intensity have rotated to the dayside of the SNOE track some hours after 1245 UT. On the basis of studies of substorm events, we can expect that most of the precipitation associated with possible substorm expansions after 1245 UT occurs on the nightside around geomagnetic midnight [e.g., *Østgaard et al.*, 1999]. The NO produced by this new energy input is thus not expected to be transported to the areas beneath the next SNOE passes in the late morning sector. We assume that any NO production caused by precipitation after 1245 UT, occurring locally in the late morning sector, is insignificant compared to the amount of NO produced in this geographic area during the many hours before 1245 UT. Thus we include the three SNOE passes after 1245 UT in our

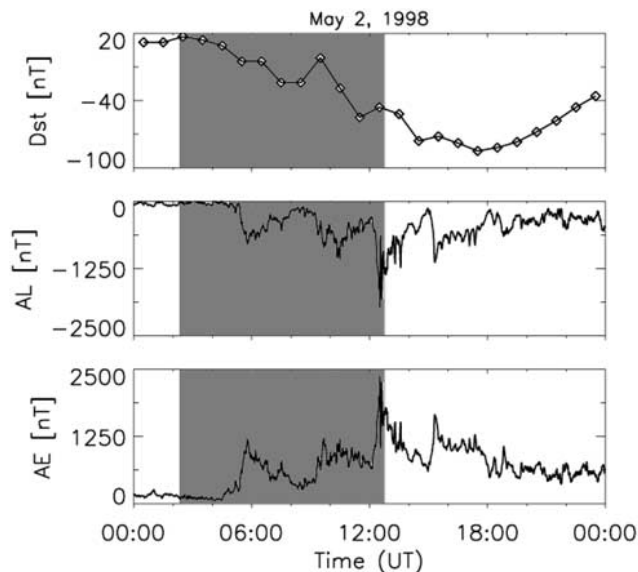


Figure 1. Dst, AL, and AE indexes for 2 May 1998. The time of PIXIE measurements is within the shaded area.

comparisons. This assumption may lead to a slightly overestimate of the production efficiency of NO.

[20] As we see from Figure 2 it takes some hours before the areas with extensive amounts of X-ray intensity have rotated to the dayside of the SNOE track. In Figure 3 we compare the NO volume density at the height of maximum density, 110 km, with the time-integrated X-ray intensity under the SNOE trajectory. Each plot corresponds to an image in Figure 2. The axis values for the NO-density and the X-ray intensity are chosen so that the data have similar amplitudes at maximum values.

[21] In the first two passes, 0405 and 0535 UT (corresponding to the upper left and middle plot in Figure 3), there are no substantial amounts of X rays observed. However, there is a minor peak in the NO density at higher latitudes. The NO density at lower latitudes is approximately $0.5-1 \times 10^8 \text{ cm}^{-3}$, and at higher latitudes it reaches $\sim 1.5 \times 10^8 \text{ cm}^{-3}$ for these two passes. In the third pass (upper right plot in Figure 3) the areas beneath the SNOE satellite have some minor amounts of integrated X-ray intensity. Because of the excess amount of NO already existing at higher latitudes, the integrated X-ray intensity needs to be somewhat larger than for the areas beneath the 0715 pass, before we in this case can see the direct response in the NO density.

[22] For the SNOE passes at 1025 UT and onward there is a distinct increase in NO at latitudes close to the X-ray intensity peak. There is a displacement between the NO and X-ray curves which will be commented upon further when discussing the energy profiles of the electron precipitation. The shape of the curves for the four last plots are quite similar.

[23] PIXIE provides X-ray measurements for 63 energy channels. To obtain sufficient count rates, the channels have been binned in six energy bands; four for the low-energy section of PIXIE, and two for the high-energy section of the detector [*Østgaard et al.*, 2000]. From the time-integrated X-ray data we can derive electron spectra. The method used involves a look-up table provided by a coupled electron-

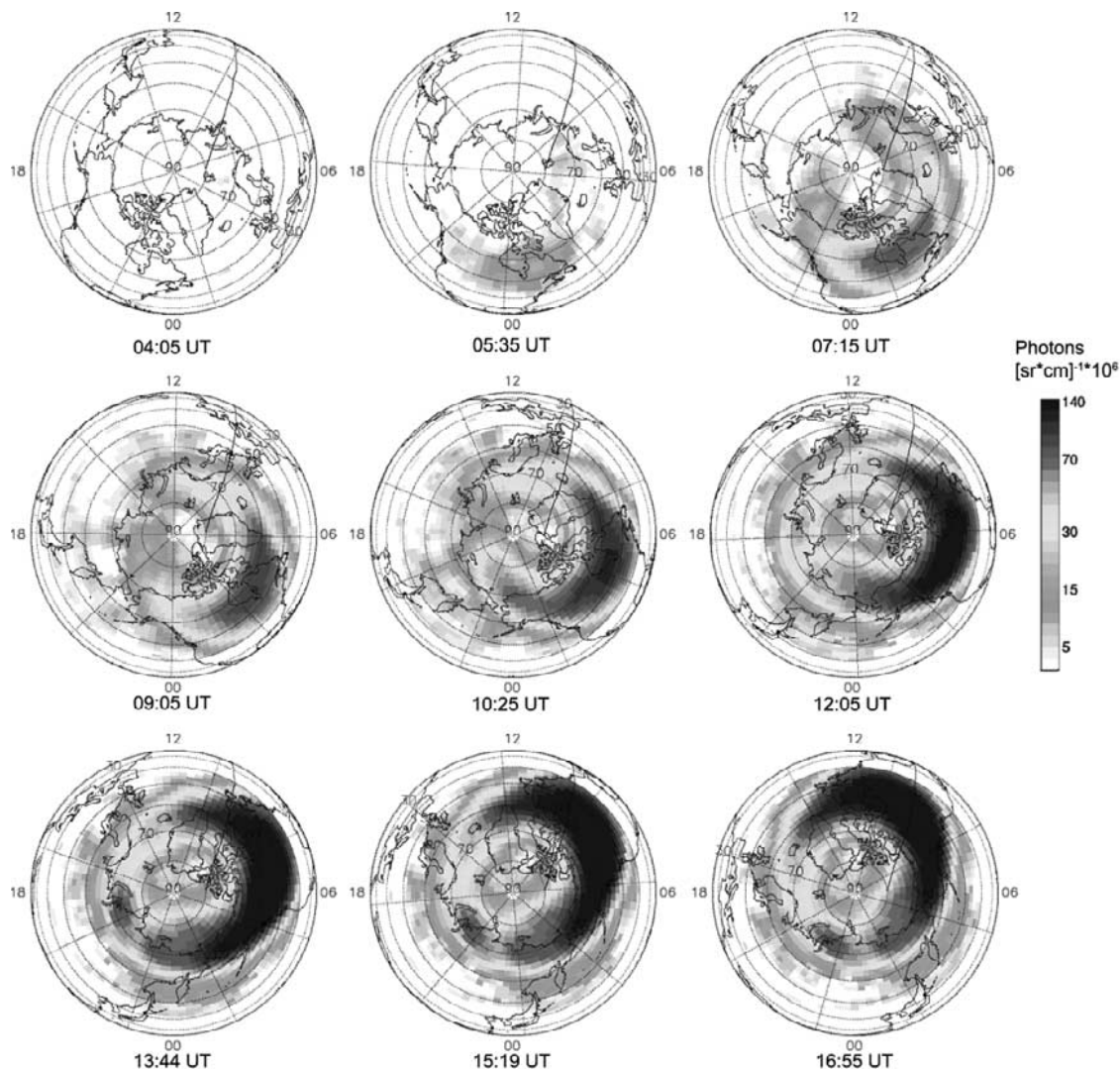


Figure 2. X-ray intensity (2.47–9.06 keV) integrated over consecutive longer intervals of time on 2 May 1998. The time displayed beneath each image is the approximate time for the current SNOE passage. For the six upper images the X-ray intensity is integrated from 0220 UT to the time of the current SNOE pass. In the three lower images the X-ray integration is from 0220 to 1245 UT. See color version of this figure at back of this issue.

photon transport code originally derived from neutron transport codes [Lorence, 1992]. Here the transport is of electrons and photons. Bremsstrahlung production, Compton scattering, photoabsorption, and secondary electron radiation are also included in the code. The look-up table, assuming isotropic electron precipitation, gives us the X-ray production emitted at different zenith angles for electron spectra of exponential shape. By using this look-up table, we have fitted the shape of the electron spectrum, which gives an X-ray spectrum corresponding to the one observed. This technique is described more thoroughly in the work of Østgaard *et al.* [2000] and has been validated by comparison with in situ DMSP electron spectra [Østgaard *et al.*, 2001].

[24] We can use the electron spectra to calculate the time-integrated energy deposition of the electron precipitation as a function of altitude. In these calculations we have used the cosine-dependent IDH (Isotropic over the Downward Hemisphere) model of Rees [1963] (also described by Rees [1989]).

[25] We have calculated electron spectra for boxes of 5° latitude and 12° longitude under the five last SNOE passes. We ended up with 25 spectra that was of reliable quality. Figure 4 shows the electron spectra calculated for four areas, from 45°N to 65°N , under the SNOE pass at 1655 UT. The electron spectra change considerably from one area to another. The energy deposition calculated from these four electron spectra, and the NO volume density as a function of height, are shown in Figure 5. The altitudes of peak intensities for the two data sets correspond fairly well. The maxima occur between 100 and 113 km altitude and differ with only ~ 4 km. The energy deposition profile is somewhat wider than the NO profile, especially above the peak. This can be explained by the lack of information about electrons with energies less than a few keV, when deriving electron fluxes from the X-ray measurements. This results in a significant uncertainty in the fluxes of the low-energy electrons, which deposit their energy at heights above the peak.

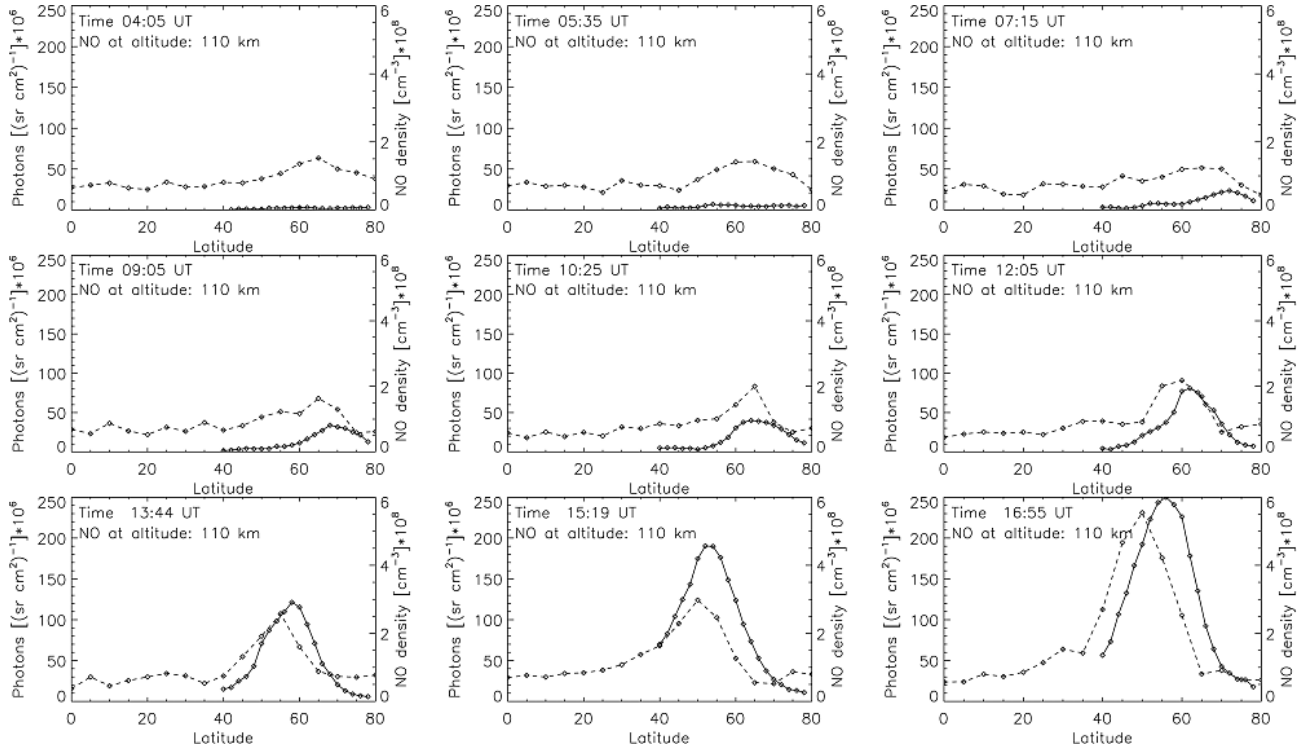


Figure 3. NO volume density (dashed line) at 110 km altitude, and time-integrated X-ray intensity (solid line) (2.47–9.06 keV) under the different SNOE passages on 2 May 1998. In the upper six plots the X-ray intensity is time-integrated from 0220 UT to the time of the current SNOE pass (the time displayed in each panel). For the three lower plots the X-ray intensity is integrated from 0220 to 1245 UT.

[26] The energy deposition and NO density as a function of latitude for the 1655 UT passage is shown in Figure 6 for different altitudes. The curves have similar shape, but above 100 km the NO density peak is displaced equatorward with respect to the peak in the energy deposition. Because of the long lifetime of NO the effects of neutral winds during the night and morning hours can lead to significant displacement from the origin of production. Studies done by *Brekke et al.* [1994] and *Nozawa and Brekke* [1995] show that for summer, at altitudes between 100 and 125 km, the neutral horizontal wind is equatorward between midnight and

morning. In the altitude range 95 to 100 km the neutral wind is poleward for these local times [*Brekke et al.*, 1994]. In Figure 6 at 96 and 100 km there is no distinct displacement of the NO maximum.

[27] On the basis of the 25 energy deposition profiles that have been deduced, the relation between the observed NO volume density and the time-integrated energy deposition is plotted in Figure 7 for the typical altitude of the peak values, 106 km. The linear fit to the data at 106 km has a slope of 8.0 NO molecules produced per keV deposited energy, and the correlation coefficient is 0.91.

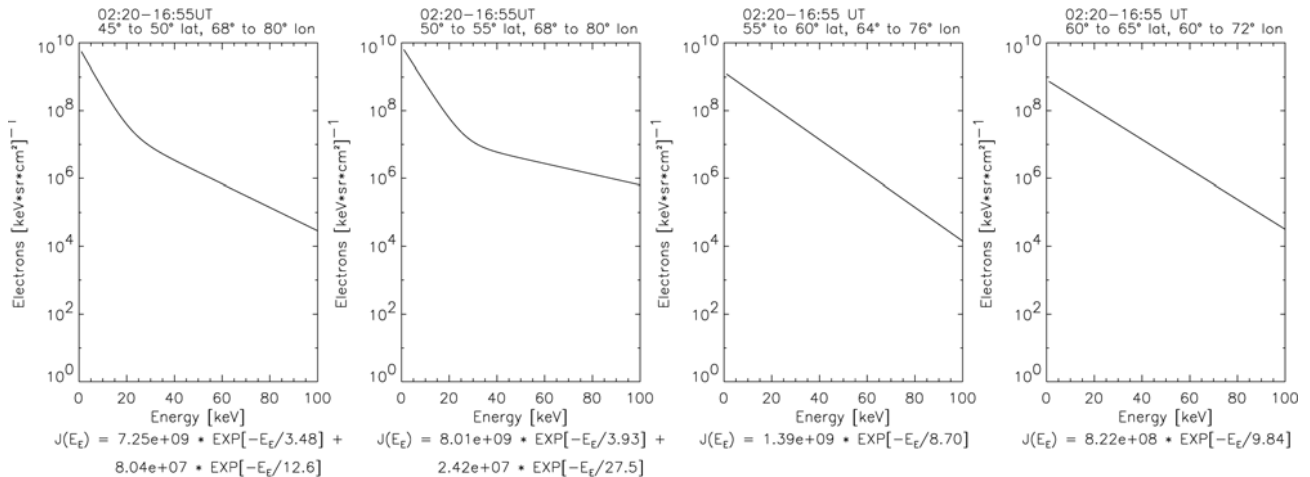


Figure 4. Calculated electron energy spectra under the SNOE pass 1655 UT on 2 May 1998.

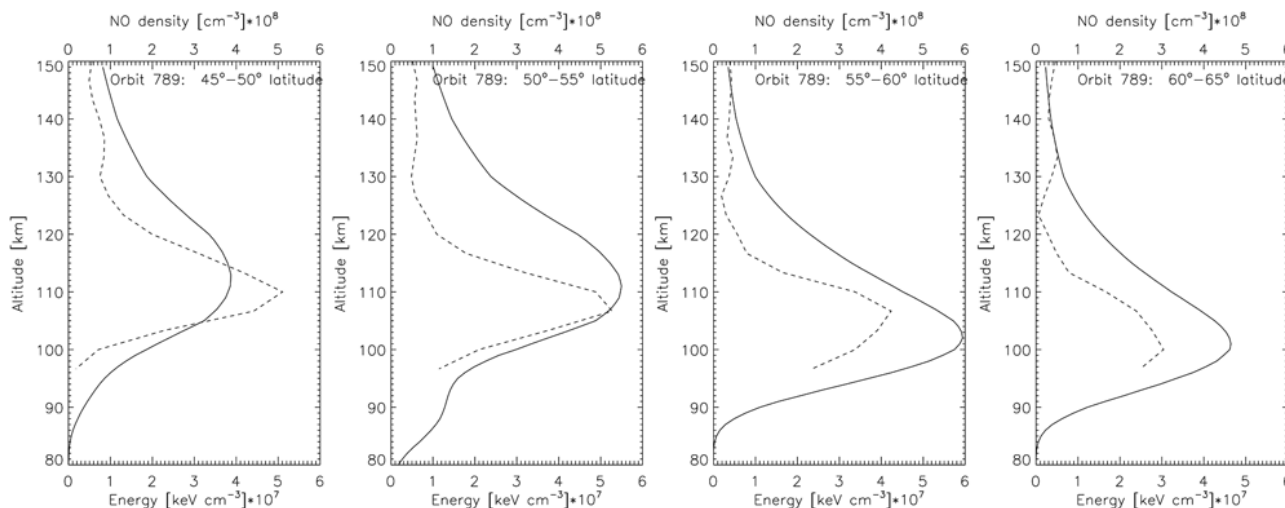


Figure 5. NO volume density (dashed line) and time-integrated electron energy deposition (solid line) under the SNOE pass 1655 UT on 2 May 1998.

[28] In Table 1 the correlation coefficients and the slopes for the linear fits are listed for different altitudes. The best correlation between the time-integrated energy deposition and the NO density is at 103 and 106 km altitude.

4. Discussion and Conclusion

[29] The development of the nitric oxide abundance at higher latitudes during the start of a geomagnetic storm event on 2 May 1998, has been compared directly with the time-integrated X-ray bremsstrahlung and with the energy

deposited by the precipitating energetic electrons. Owing to a lifetime of NO of approximately one day, and measurements of NO on the dayside only, the X-ray bremsstrahlung intensities have been integrated in geographical boxes over consecutive longer intervals of time. This enables us to study the accumulation effects of the electron precipitation on the NO concentration.

[30] Although the geomagnetic conditions were quiet the day before the storm, there was some excess NO density at higher latitudes before the onset of the storm. Thus we do not see any direct increase in NO for lower X-ray intensi-

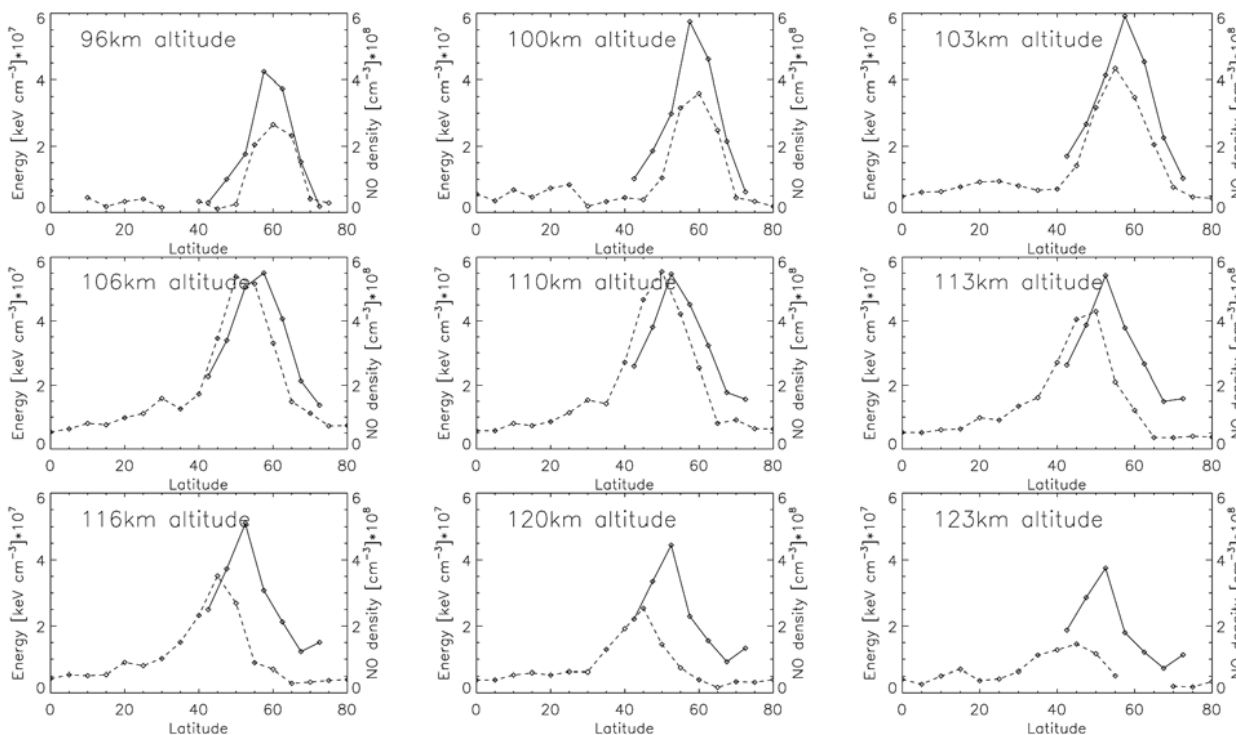


Figure 6. NO volume density (dashed line) and time-integrated electron energy deposition (solid line) under the SNOE pass 1655 UT on 2 May 1998.

ties. The X-ray intensities and energy deposition are in good agreement with the NO density concerning the altitude of maximum values and the shape of the profiles. There is a displacement of the NO profile equatorward compared with the electron energy deposition at altitudes above 100 km. The displacement is probably caused by neutral horizontal winds. With a lifetime of ~ 1 day the wind effects on nitric oxide will be substantial for time periods of many hours as used in this study.

[31] The relation between the NO volume density and the energy deposition is found to be linear. The best correlation (>0.90) is at 103 and 106 km altitude for the event of 2 May 1998, where $\sim 83\%$ of the NO is produced by electron precipitation. With the technique used in this study, where the electron energy deposition is computed from electron energy spectra, that are found from X-ray bremsstrahlung energy spectra, we find the net NO production at 106 km altitude to be 8.0 molecules per keV deposited energy. The average altitude of the peak values of both NO and precipitating electron energy is found to be 106 km. These results are obtained assuming that the NO produced by the electron precipitation that may occur between 1245 and 1655 UT will not be detected for the SNOE orbits in this time interval. This may cause the production efficiency to be slightly overestimated. We have further assumed that the loss of NO is negligible for the time scale of this study. This assumption can cause an underestimate of the NO production per energy deposited.

[32] The correlation between the NO volume density and electron precipitation found in this study is in agreement with previous theoretical predictions; the profile of the NO density resembles the profile of the energetic electron energy deposition fairly well. The linear relation between the two data sets, and the production rate is not easily comparable to earlier results. Previous model calculations [e.g., *Bailey et al.*, 2002; *Barth*, 1992] assume constant electron precipitation over several days. *Bailey et al.* [2002] operate with an aurora of constant energy flux of 1 mW m^{-2} and a characteristic energy of 4 keV, turned on for 4 whole days. Their model gives the equilibrium NO produced under constant conditions. In the present paper we study the

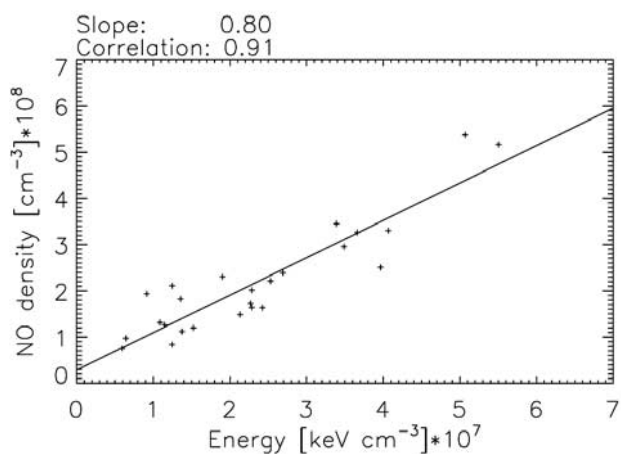


Figure 7. NO volume density versus energy deposition at 106 km altitude. The slope of the linear fit is 8.0 molecules/keV.

Table 1. Table of the Slope and Correlation Coefficients for the Linear Fit to the NO Densities and Energy Deposition at Different Altitudes

Altitude, km	Slope, 10 keV^{-1}	Correlation
120	0.35	0.67
116	0.51	0.74
113	0.68	0.79
110	0.84	0.86
106	0.80	0.91
103	0.64	0.92
100	0.53	0.82
96	0.47	0.75

effects of energetic electron precipitation on the NO concentration from the start of an active period with strong temporal and spatial variations in the precipitation. Thus our results cannot be directly compared with the results from the above mentioned calculations.

[33] As mentioned above, we find a linear relationship between the NO production and the deposited energy. According to several other studies [e.g., *Codrescu et al.*, 1997; *Bailey et al.*, 2002], the relation between the NO density and the electron energy deposition rate is not linear. When the energy flux increases, the NO density reaches a level of saturation [*Bailey et al.*, 2002, Figure 11]. For this present study the intensity of the time-integrated electron precipitation is too small for the integrated energy deposition to reach values that cohere with the saturation of NO.

[34] We see transport effects of the NO in the north-south direction. However, we find a 0.90 correlation between the NO density and the electron energy deposition. The reason for this high correlation is probably the fairly large areas, 5° latitude times 12° longitude, for which the energy deposition has been calculated.

[35] In future works it would be interesting to include information of the neutral wind, both horizontal and vertical winds. In addition the energy range of the electron energy spectra would be extended if UV measurements from the Ultraviolet Imager (UVI) on board the Polar satellite were included. This would give a better determination of the low energy part of the electron spectrum and thereby more precise energy deposition profiles at higher altitudes.

[36] **Acknowledgments.** The Norwegian authors would like to thank the Norwegian Research Council for financial support. We also thank D. L. Detrick and T. J. Rosenberg at the University of Maryland for providing us with a computer code to derive the electron energy deposition.

[37] Arthur Richmond thanks Linwood Callis and Raymond Roble for their assistance in evaluating this paper.

References

- Bailey, S. M., C. A. Barth, and S. C. Solomon (2002), A model of nitric oxide in the lower thermosphere, *J. Geophys. Res.*, *107*(8), 1205, doi:10.1029/2001JA000258.
- Baker, D. N., C. A. Barth, K. E. Mankoff, S. G. Kanekal, S. M. Bailey, G. M. Mason, and J. E. Mazur (2001), Relationships between precipitating auroral zone electrons and lower thermospheric nitric oxide densities: 1998–2000, *J. Geophys. Res.*, *106*, 24,465.
- Barth, C. A. (1992), Nitric oxide in the lower thermosphere, *Planet. Space Sci.*, *40*, 315.
- Barth, C. A., S. M. Bailey, and S. C. Solomon (1999), Solar-terrestrial coupling: Solar soft x-rays and thermospheric nitric oxide, *Geophys. Res. Lett.*, *26*, 1251.
- Barth, C. A., D. N. Baker, K. D. Mankoff, and S. M. Bailey (2001), The northern auroral region as observed in nitric oxide, *Geophys. Res. Lett.*, *28*, 1463.

- Barth, C. A., D. N. Baker, K. D. Mankoff, and S. M. Bailey (2002), Magnetospheric control of the energy input into the thermosphere, *Geophys. Res. Lett.*, *29*(13), 1629, doi:10.1029/2001GL014362.
- Barth, C. A., K. D. Mankoff, S. M. Bailey, and S. C. Solomon (2003), Global observations of nitric oxide in the thermosphere, *J. Geophys. Res.*, *108*(A1), 1027, doi:10.1029/2002JA009458.
- Brekke, A., S. Nozawa, and T. Sparr (1994), Studies of the *E*-region neutral wind in the quiet auroral ionosphere, *J. Geophys. Res.*, *99*, 8801.
- Callis, L. B., and J. D. Lambeth (1998), NO_y formed by precipitating electron events in 1991 and 1992: Descent into the stratosphere as observed by ISAMS, *Geophys. Res. Lett.*, *25*, 1875.
- Callis, L. B., D. N. Baker, M. Natarajan, J. B. Blake, R. A. Mewaldt, R. S. Selesnick, and J. R. Cummings (1996), A two-dimensional model simulation of downward transport of NO_y into the stratosphere: Effects of the 1994 austral spring O₃ and NO_x, *Geophys. Res. Lett.*, *23*, 1905.
- Callis, L. B., M. Natarajan, D. S. Evans, and J. D. Lambeth (1998), Solar atmospheric coupling by electrons (SOLACE): 1. Effects of the May 12, 1997, solar event on the middle atmosphere, *J. Geophys. Res.*, *103*, 28,405.
- Codrescu, M. V., T. J. Fuller-Rowell, R. G. Roble, and D. S. Evans (1997), Medium energy particle precipitation influences on the mesosphere and lower thermosphere, *J. Geophys. Res.*, *102*, 19,977.
- Crowley, G., A. Ridley, D. Winningham, R. Frahm, J. Sharber, J. Russel, and R. G. Roble (1998), Nitric oxide variations in the mesosphere and lower thermosphere during the November 1993 storm period, *J. Geophys. Res.*, *103*, 26,395.
- Crowley, G., A. Ridley, D. Winningham, R. Frahm, J. Sharber, J. Russel, and R. G. Roble (1999), On the hemispheric symmetry in thermospheric nitric oxide, *Geophys. Res. Lett.*, *26*, 1545.
- Imhof, W. L., et al. (1995), The Polar Ionospheric X-ray Imaging Experiment (PIXIE), *Space Sci. Rev.*, *71*, 385.
- Lorenz, L. J. (1992), CEPXS/ONELD version 2.0: A discrete ordinates code package for general one-dimensional coupled electron-photon transport, *IEEE Trans. Nucl. Sci.*, *39*(4), 1031.
- Nozawa, S., and A. Brekke (1995), Studies of the *E* region neutral wind in the disturbed auroral ionosphere, *J. Geophys. Res.*, *100*, 14,171.
- Østgaard, N., J. Stadsnes, J. Bjordal, R. R. Vondrak, S. A. Cummer, D. L. Chenette, G. K. Parks, M. J. Brittner, and D. L. McKenzie (1999), Global-scale electron precipitation features seen in UV and X-rays during substorms, *J. Geophys. Res.*, *104*, 10,191.
- Østgaard, N., J. Stadsnes, J. Bjordal, R. R. Vondrak, S. A. Cummer, D. L. Chenette, M. Schultz, and J. G. Pronko (2000), Cause of the localized maximum of X-ray emission in the morning sector: A comparison with electron measurements, *J. Geophys. Res.*, *105*, 20,869.
- Østgaard, N., J. Stadsnes, J. Bjordal, G. A. Germany, R. R. Vondrak, G. K. Parks, S. A. Cummer, D. L. Chenette, and J. G. Pronko (2001), Auroral electron distributions derived from combined UV and X-ray emissions, *J. Geophys. Res.*, *106*, 26,081.
- Petrinec, S. M., W. L. Imhof, C. A. Barth, K. D. Mankoff, D. N. Baker, and J. G. Luhmann (2003), Comparison of thermospheric high-latitude nitric oxide observations from SNOE and global auroral X-ray bremsstrahlung from PIXIE, *J. Geophys. Res.*, *108*(A3), 1123, doi:10.1029/2002JA009451.
- Randall, C. E., D. E. Siskind, and R. M. Bevilacqua (2001), Stratospheric NO_x enhancements in the Southern Hemisphere vortex in winter/spring of 2000, *Geophys. Res. Lett.*, *28*, 2385.
- Rees, M. H. (1963), Auroral ionization and excitation by incident energetic electrons, *Planet. Space Sci.*, *11*, 1209.
- Rees, M. H. (1989), *Physics and Chemistry of the Upper Atmosphere*, Cambridge Univ. Press, New York.
- Ridley, A. J., G. Crowley, R. Frahm, D. Winningham, J. Sharber, J. Russel, and R. G. Roble (1999), Variations of the nitric oxide mass mixing ratio in the thermosphere as a function of Kp, *Geophys. Res. Lett.*, *26*, 1541.
- Roble, R. G. (1992), The polar lower thermosphere, *Planet. Space Sci.*, *40*, 271.
- Siskind, D. E., C. A. Barth, D. S. Evans, and R. G. Roble (1989), The response of thermospheric nitric oxide to an auroral storm: 2. Auroral latitudes, *J. Geophys. Res.*, *94*, 16,899.
- Solomon, S. C., P. J. Crutzen, and R. G. Roble (1982), Photochemical coupling between the thermosphere and lower atmosphere: 1. Odd nitrogen from 50 to 120 km, *J. Geophys. Res.*, *87*, 7206.
- Solomon, S. C., et al. (1996), The student nitric oxide explorer, *Proc. SPIE Int. Soc. Opt. Eng.*, *2810*, 121.
- Solomon, S. C., C. A. Barth, and S. M. Bailey (1999), Auroral production of nitric oxide measured by the SNOE satellite, *Geophys. Res. Lett.*, *26*, 1259.

A. Aksnes, H. Nesse, C. Sætre, and J. Stadsnes, Department of Physics and Technology, University of Bergen, Allégaten 55, N-5007 Bergen, Norway. (arve.aksnes@ift.uib.no; hilde.nesse@ift.uib.no; camilla.satre@ift.uib.no; johan.stadsnes@ift.uib.no)

D. N. Baker and C. A. Barth, Laboratory for Atmospheric and Space Physics, Boulder, CO 80303-7814, USA. (baker@lasp.colorado.edu; charles.barth@lasp.colorado.edu)

N. Østgaard, Space Sciences Laboratory, University of California, Berkeley, CA 94720-7450, USA. (nikost@ssl.berkeley.edu)

S. M. Petrinec, Lockheed Martin Advanced Technology Center, Palo Alto, CA 94304-1181, USA. (petrinec@mail.spasci.com)

R. R. Vondrak, NASA/Goddard Space Flight Center, Greenbelt, MD 20771, USA. (richard.vondrak@gsfc.nasa.gov)

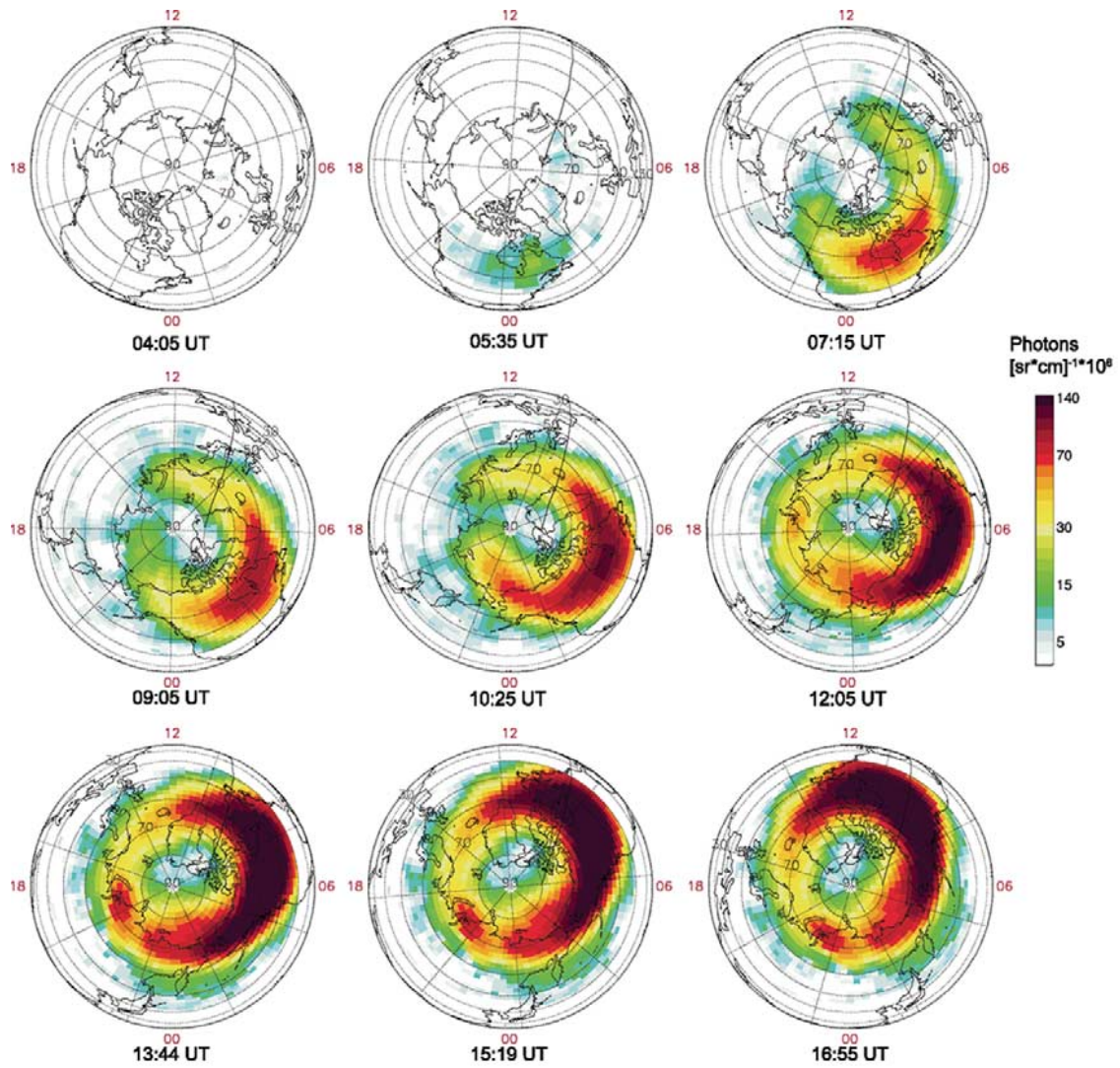


Figure 2. X-ray intensity (2.47–9.06 keV) integrated over consecutive longer intervals of time on 2 May 1998. The time displayed beneath each image is the approximate time for the current SNOE passage. For the six upper images the X-ray intensity is integrated from 0220 UT to the time of the current SNOE pass. In the three lower images the X-ray integration is from 0220 to 1245 UT.

